Cochlear synaptopathy impairs suprathreshold tone-in-noise coding in the cochlear nucleus

A. Hockley[1,2], L. R. Cassinotti[1], M. Selesko[1], G. Corfas[1] and S. E. Shore[1,3,4]

[1] *Kresge Hearing Research Institute, Department of Otolaryngology, University of Michigan, Ann Arbor, MI, USA*
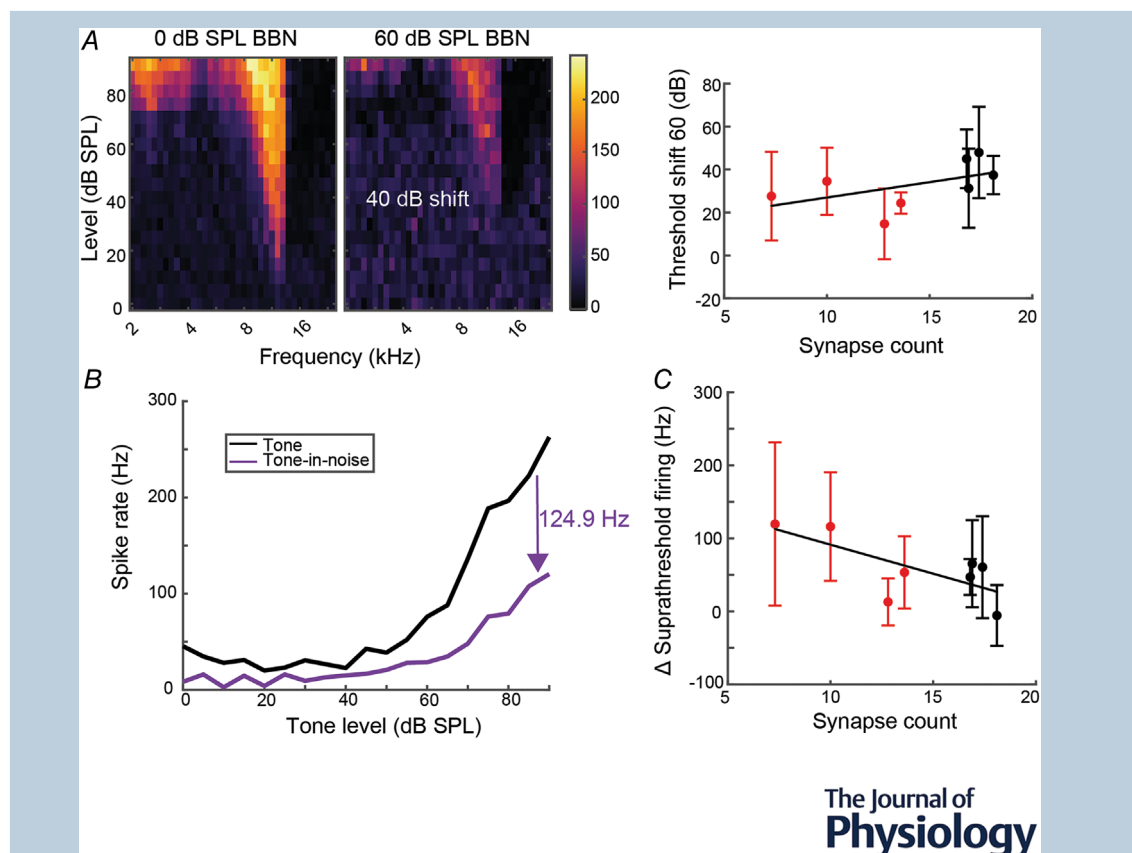[2] *Instituto de Neurociencias de Castilla y León, Universidad de Salamanca, Salamanca, Spain*
[3] *Department of Molecular and Integrative Physiology, University of Michigan, Ann Arbor, MI, USA*
[4] *Department of Biomedical Engineering, University of Michigan, Ann Arbor, MI, USA*

The Journal of Physiology

Abstract Hearing impairment without threshold elevations can occur when there is damage to high-threshold auditory nerve fibre synapses with cochlear inner hair cells. Instead, cochlear synaptopathy produces suprathreshold deficits, especially in older patients, which affect conversational speech. Given that listening in noise at suprathreshold levels presents significant challenges to the ageing population, we examined the effects of synaptopathy on tone-in-noise coding on the central recipients of auditory nerve fibres, i.e. the cochlear nucleus neurons. To induce synaptopathy, guinea pigs received a unilateral sound overexposure to the left ears. A separate group received sham exposures. At 4 weeks post-exposure, thresholds had recovered but reduced auditory brainstem response wave 1 amplitudes and auditory nerve synapse loss remained on the left side. Single-unit responses were recorded from several cell types in the ventral cochlear nucleus to

pure-tone and noise stimuli. Receptive fields and rate–level functions in the presence of continuous broadband noise were examined. The synaptopathy-inducing noise exposure did not affect mean unit tone-in-noise thresholds, nor the tone-in-noise thresholds in each animal, demonstrating equivalent tone-in-noise detection thresholds to sham animals. However, synaptopathy reduced single-unit responses to suprathreshold tones in the presence of background noise, particularly in the cochlear nucleus small cells. These data demonstrate that suprathreshold tone-in-noise deficits following cochlear synaptopathy are evident in the first neural station of the auditory brain, the cochlear nucleus neurons, and provide a potential target for assessment and treatment of listening-in-noise deficits in humans.

Corresponding author S. E. Shore: Department of Otolaryngology, University of Michigan, 1150 West Medical Centre Drive, Ann Arbor, MI 48109, USA.   Email: sushore@umich.edu

Abstract figure legend *A*, unilateral noise exposure induces synaptopathy and temporary threshold shift (TTS) in guinea pigs. *B*, auditory thresholds of single units in the cochlear nucleus are shifted in background noise, and this shift is not affected by synaptopathy. *C*, suprathreshold firing rates are decreased by background sound, and this decrease is correlated with cochlear synaptopathy.

Key points

- Recording from multiple central auditory neurons can determine tone-in-noise deficits in animals with quantified cochlear synapse damage.
- Using this technique, we found that tone-in-noise thresholds are not altered by cochlear synaptopathy, whereas coding of suprathreshold tones-in-noise is disrupted.
- Suprathreshold deficits occur in small cells and primary-like neurons of the cochlear nucleus.
- These data provide important insights into the mechanisms underlying difficulties associated with hearing in noisy environments.

Introduction

Hearing deficits can occur in the absence of auditory threshold shifts when preferential injury occurs to the synapses of low-spontaneous rate (SR), high-threshold auditory nerve fibres (ANFs) with cochlear inner hair cells (IHCs) (Furman et al., 2013). High-threshold ANFs can be identified by their contacts on the modiolar side of IHCs and are calretinin rich (Sharma et al., 2018). Cochlear synaptopathy is a potentially widespread health issue, because human temporal bones demonstrate broad synaptic damage across an ageing population, even before hair cell damage (Makary et al., 2011; Viana et al., 2015; Wu et al., 2019). Furthermore, age is negatively correlated with the ability to understand speech in noisy environments, even in subjects with clinically normal auditory thresholds (Pichora-Fuller & Souza, 2003; Rajan & Cainer, 2008; Robert Frisina & Frisina, 1997).

Aged patients with normal audiometric thresholds, but presumably more cochlear synaptopathy, have worse tone-in-noise (TIN) thresholds than young healthy

Adam Hockley received his PhD at the Institute of Hearing Research in Nottingham, UK. Here, Adan learned about auditory brainstem physiology while studying the role of nitric oxide in the cochlear nucleus in tinnitus. From here, he moved to the Shore Lab at the University of Michigan and began to focus on intensity coding within the small cell cap of the cochlear nucleus. He has found important intensity-coding abilities in this area and hopes to study these more in the future, assessing how brainstem circuits are altered by auditory pathologies. **Susan E. Shore** received her PhD in Physiology from LSU medical school, where her work focused on cochlear mechanics. Her postdoctoral work at University of Pittsburgh and University of Michigan focused on complex signal processing in the brainstem. She is currently Professor at the University of Michigan Kresge Hearing Institute, where her work focuses on multisensory integration and neural plasticity in the central auditory system and its influence after hearing loss and tinnitus.

hearing patients (Ralli et al., 2019). Therefore, TIN tests have been considered as viable tests for synaptopathy. Using a TIN test has the advantage of being able to determine frequency-specific deficits without requiring complex higher-level processes, such as attention, and it can be standardized globally across different languages. The alternative, speech-in-noise tests, use stimuli most often described as difficult by likely cochlear synaptopathy patients; however, they have had limited success as a synaptopathy test in human studies, possibly owing to the attention required (Couth et al., 2020; Guest et al., 2018).

Animal studies are useful to determine perceptual consequences of cochlear synaptopathy, because the peripheral damage can be carefully titrated and measured, allowing correlations with changes to auditory processing (as in the study by Parthasarathy & Kujawa, 2018). Mice with ouabain-induced neural degeneration in the cochlea have shown increased behavioural TIN detection thresholds, despite no changes to tone-in-quiet thresholds (Resnik & Polley, 2021). In contrast, in a budgerigar model using kainite to induce auditory-nerve synapse loss, no changes to behavioural TIN thresholds were seen (Henry & Abrams, 2021). These studies leave open the question of how a noise-induced cochlear synaptopathy might affect TIN coding.

Here, we record from cochlear nucleus (CN) neurons in guinea pigs with cochlear synaptopathy and demonstrate that the peripheral cochlear neural damage does not produce TIN threshold shifts. Furthermore, our recordings show that suprathreshold TIN is impaired, providing a potential target for detection of cochlear synaptopathy in humans. These data provide important insights into mechanisms underlying perceptual difficulties accompanying synaptopathy.

Methods

Ethical approval

All animal experimental procedures were performed under protocols established by the National Institutes of Health (publication 80-23) and were approved by the institutional animal care and use committee at the University of Michigan. Male and female ($n = 8$ and 6, respectively) pigmented guinea pigs weighing $280-500$ g were obtained from Elm Hill Labs. No differences in unit responses between sex were found. Guinea pigs were housed in pairs on a 12 h–12 h light–dark cycle, with food and water available *ad libitum*. Using a unilateral noise exposure on the left side, 10 guinea pigs (six male and four female) were noise exposed to produce cochlear synaptopathy. A further four animals (two male and two female) underwent a sham exposure to act as a control group.

Noise exposure and auditory brainstem responses

Auditory brainstem responses (ABRs; the volume-conducted synchronous activity of ANFs and their brainstem recipients in response to short tone bursts) were recorded from guinea pigs anaesthetized with a mixture of ketamine (50 mg kg^{-1}, s.c.; Hospira, Lake Forest, IL, USA) and xylazine (5 mg kg^{-1}, s.c.; Akorn, Lake Forest, IL, USA). Anaesthetic depth was monitored using the rear paw withdrawal reflex and maintained using 10 mg kg^{-1} ketamine and 1 mg kg^{-1} xylazine supplements. Atropine (0.05 mg kg^{-1}, IP (intraperitaneally)) was administered to reduce bronchial secretions. Animals were placed in a stereotaxic frame (Kopf, Tujunga, CA, USA) within a sound-attenuating and electrically shielded double-walled chamber. Three needle electrodes were placed into the skin, one at the dorsal midline close to the neural crest, one behind the left pinna, and one behind the right pinna.

Auditory brainstem responses were recorded in response to tone bursts [8, 12, 16 and 20 kHz; 5 ms duration, 1 ms rise/fall times, 21 Hz presentation rate, 512 repetitions in 10 dB steps from 0 to 90 dB sound pressure level (SPL); RZ6, Tucker-Davis Technologies (TDT), Alachua, FL, USA]. The ABR wave 1 amplitudes were analysed with TDT BioSigRZ. Auditory brainstem responses were recorded before (baseline) and immediately after noise exposure and at 2 and 4 weeks post-exposure.

For noise trauma, anaesthetized animals were unilaterally exposed (left ear) to narrow-band noise (centred at 7 kHz, half-octave bandwidth) at 102 dB SPL for 2 h. Sham-exposed animals underwent the same procedures, without turning on the noise.

Single-unit surgery and sound presentation

At the 4 week time point, immediately after ABR recordings, single-unit recordings were made in the CN. Guinea pigs were anaesthetized with ketamine (50 mg kg^{-1}, s.c.; Hospira) and xylazine (5 mg kg^{-1}, s.c.; Akorn). Anaesthetic depth was monitored using the rear paw withdrawal reflex and maintained using 10 mg kg^{-1} ketamine and 1 mg kg^{-1} xylazine supplements. Atropine (0.05 mg kg^{-1}, IP) was administered during the initial surgery to reduce bronchial secretions. Animals were placed in a stereotaxic frame (Kopf) within a sound-attenuating and electrically shielded double-walled chamber. A midline incision was made to expose the skull. The temporalis muscle was removed, and a craniotomy was performed to allow access to the left cerebellum. The dura mater was removed, and the exposed brain surface was kept moist by regular applications of saline. Auditory stimuli were delivered monaurally via a closed-field, calibrated system (modified

DT770 drivers; Beyerdynamic, Heilbronn, Germany) coupled to hollow ear bars. The speakers were driven by a TDT System 3 (RZ6, PA5 and HB7), controlled by TDT Synapse and custom MATLAB (Mathworks, Natick, MA, USA) software.

Neural recordings

Multichannel recording probes (NeuroNexus; Ann Arbor, MI, USA) were advanced stereotaxically through the cerebellum towards the left CN using an MP-285 microdrive (Sutter Instruments, Novato, CA, USA). Signals were amplified by a TDT PZ5 preamplifier connected to a TDT RZ2 processor for filtering (0.3–5 kHz), and data were collected using TDT Synapse software. Spikes were detected online, with the threshold set at four standard deviations from mean background noise, then spike-sorted *post hoc* using principal components analysis (PCA) clustering of spike waveforms. Electrodes were positioned such that shanks passed through the dorsal cochlear nucleus (DCN) to reach the small cell cap (SCC) and ventral cochlear nucleus (VCN). Units were typed by their temporal responses [peristimulus time histograms (PSTHs)] to tone-burst and broadband noise (BBN), receptive fields (RFs) and rate–level functions (RLFs) (Ghoshal & Kim, 1997; Palmer, 1987; Stabler et al., 1996; Winter & Palmer, 1995). Units were characterized further using a machine learning model described previously (Hockley et al., 2022), which divided units into five broad categories; PL (bushy cells), Ch (T-stellates), SC (small cells), B (buildups) and On (onsets). Receptive-field stimuli consisted of randomized tone bursts (50 ms duration, 200 ms interstimulus interval, 2−24 kHz, 0.1 octave spacing, 5 dB steps, 5 ms cosine on/off ramp, 15 repeats, randomized). From these, thresholds and characteristic frequencies (CFs) were obtained from the lowest sound level and frequency to produce spikes more than two standard deviations above spontaneous firing rates. Rate–level functions at the CF were then used for further analyses. Receptive fields were collected in silence or in the presence of a continuous 40 or 60 dB SPL broadband background noise. After neurophysiological recordings, animals were killed (1 ml Euthatal, Sodium Pentobarbital. Duggan Veterinary Supplies Ltd (IP)) and the cochleae collected.

Cochlear immunostaining for synaptic counts

Four weeks after noise exposure, after the final ABRs and neural recordings, guinea pigs were perfused with 500 ml PBS followed by 500 ml 4% paraformaldehyde. After perfusion, the inner ear tissues were dissected and postfixed in 4% paraformaldehyde in 0.01 M PBS for 2 h at room temperature, followed by decalcification

in 5% EDTA at 4°C for 3 weeks. Fresh 5% EDTA was provided weekly. Cochlear tissues were microdissected and permeabilized by freeze–thawing in 30% sucrose. The microdissected tissues were incubated in blocking buffer containing 5% normal horse serum and 0.3% Triton X-100 in PBS for 1 h. Tissues were then incubated in primary antibodies (diluted in 1% normal horse serum and 0.3% Triton X-100 in PBS) at 37°C overnight. The primary antibodies used in this study were as follows: anti-Ctbp2 (BD Biosciences, San Jose, CA, USA; 1:200; catalogue no. 612 044), anti-GluR2 (Millipore, Billerica, MA, USA; 1:1000; catalogue no. MAB397) and anti-MyoVIIa (Proteus Biosciences, Ramona, CA, USA; 1:100; catalogue no. 25-6790). Tissues were then incubated with appropriate Alexa Fluor-conjugated fluorescent secondary antibodies (Invitrogen, Carlsbad, CA, USA; 1:1000 diluted in 1% normal horse serum and 0.3% Triton X-100 in PBS; AF488 IgG2a, catalogue no. A-21 131; AF568 IgG1, catalogue no. A-21 124; AF647 IgG, catalogue no. A-21 244) for 1 h at room temperature. The tissues were mounted on microscope slides in ProLong Diamond Antifade Mountant (Thermo Fisher Scientific).

Cochleae were imaged at low power ($\times 10$ magnification) to convert cochlear location into frequency (tonotopic mapping) using a custom plug-in to ImageJ (1.53c, NIH, Bethesda, MD, USA). Cochlear tissues from 12, 16 and 20 kHz regions were used for further analyses. Confocal z-stacks of cochlear tissues were obtained using a Leica SP8 confocal microscope. For IHC synapse counts, z-stacks (0.3 μm step size) were obtained under $\times 63$ ($+2.4 \times$ optical zoom) magnification spanning the entire IHC height to ensure that all synapses were imaged.

Imaging and analyses of synapses were performed as described by Wan et al. (2014). Briefly, ImageJ/Fiji software (v.1.53c; NIH) was used for image processing and quantification. One cochlea from each animal was imaged for each experiment, with three images acquired at each cochlear region. For synapse counts, CtBP2 and GluR2 puncta in each image stack were captured and counted manually using the ImageJ/Fiji software multi-point counter tool. Synaptic counts of each z-stack were divided by the number of IHCs, which could be visualized by staining with MyoVIIa antibody. Each individual image usually contained 8−10 IHCs. For figures, one representative image was selected from amongst the 24−30 images from the specific frequency shown.

Experimental design and statistical analysis

Graphics and statistical tests for ABR and synapse-count data were performed using GraphPad Prism v.9.3.1 for Windows (GraphPad Software; www.graphpad.com). Data sets with normal distributions were analysed

with parametric tests, whereas non-parametric tests were used for sets that did not conform to normality criteria. Two-way ANOVAs, followed by Tukey's multiple comparisons test were used to compare ABR thresholds and ABR wave P1 amplitudes at each time point (baseline, post-exposure/sham, 2 and 4 weeks post-exposure/sham). Quantification of confocal microscopy images for IHC synapse density at an individual frequency were analysed by Student's unpaired *t* test (Mann–Whitney *U* test). Single-unit data analysis and statistics were conducted in MATLAB. Statistical tests, including Student's unpaired *t* test, the Kruskal–Wallis test and Pearson's correlation coefficient were used to compare between groups ($\alpha = 0.05$). All average data are presented as the mean $\pm$ SD.

Results

Evidence of cochlear synaptopathy

Auditory brainstem responses immediately after acoustic trauma revealed large threshold shifts for frequencies above the noise exposure spectrum, which returned to baseline in most frequencies within 2 weeks, with a mild permanent threshold elevation at the noise-exposure frequency (Fig. 1*A*). At 12 kHz, noise exposure increased mean ABR thresholds from 7.5 (SD 4.926) to 74 (8.433) dB SPL. After 2 and 4 weeks, these thresholds reverted to 9.286 (6.075) and 11 (6.583) dB SPL, respectively. Auditory brainstem response wave 1 amplitude, representing synchronized ANF activity, was measured as a potential indicator of cochlear synaptopathy (Lobarinas et al., 2017). In contrast to the temporary nature of the threshold shifts, large noise-induced decreases in ABR wave 1 amplitudes were observed, which did not recover fully by 4 weeks post-exposure (Fig. 1*B*). At 12 kHz, noise exposure reduced the mean normalized ABR P1 amplitudes from 100 (15.241) to 12.205 (12.568) percent. After 2 and 4 weeks, these amplitudes were 74.226 (23.063) and 74.796 (23.921) percent, respectively. Sham-exposed animals showed no significant changes to ABR thresholds or wave 1 amplitudes at any time point (Fig. 1*A* and *B*). Four weeks after noise exposure, CN recordings were performed, and cochleae were processed for histological analysis. Consistent with the observed reduction in ABR wave 1 amplitudes in the exposed animals, IHC synapse densities were decreased compared with the sham group (Fig. 1*C* and *D*), demonstrating that the noise exposure was sufficient to produce IHC synaptopathy.

Cochlear nucleus recordings

Four weeks after noise exposure, 32-channel electrodes were used to isolate 699 single units from the 10 noise-exposed (NE) animals and 379 units from the four sham-exposed animals. Electrodes were positioned to record units from the SCC and VCN simultaneously. As previously described (Hockley et al., 2022), unit types were classified using a machine learning model based on their temporal and frequency response patterns, which was authenticated by manual unit typing (Ghoshal & Kim, 1997; Stabler et al., 1996; Winter & Palmer, 1995; Young et al., 1988). Onset and weakly driven units were excluded from analyses owing to their low numbers. Responses of typical small cell (SC), primary-like (PL) and chopper (Ch) neurons are shown in Fig. 2. For each cell type, the RLF, PSTH and RF from a single example unit are shown (Fig. 2 *A–C*), with the mean RLFs for that cell type for the noise- and sham-exposed groups (Fig. 2*D*). No differences in the mean RLFs were observed in the synaptopathy animals compared with the sham group. This result was unexpected, because it indicates no impairment of suprathreshold tone coding in the CN, thus challenging the hypothesis that reduced supra-threshold input following cochlear synaptopathy results in lower spike rates in the CN. Furthermore, no significant differences were found between thresholds of small cells from sham- and noise-exposed animals [sham 32.2 (SD 15.65) dB SPL, NE 32.84 (14.95) dB SPL, $n = 125$ and 169, respectively; $P = 0.947$]. Likewise, for primary-like neurons no significant differences in thresholds were observed [sham 34.8 (SD 15.17) dB SPL, NE 36.54 (14.5) dB SPL; $P = 0.353$]. And for chopper cells, a significant increase in threshold was seen [sham 16.38 (SD 11.65) dB SPL, NE 27.41 (13.74) dB SPL; $P < 0.0001$).

Primary-like spontaneous firing rates were significantly reduced by noise exposure [from 9.02 (SD 11.489) to 6.55 (10.12) Hz; $P = 0.000572$], but no significant changes were seen in small cells or chopper cells.

Cochlear nucleus suprathreshold TIN coding is impaired after synaptopathy

Although synaptopathy does not affect TIN threshold shifts in the VCN cells, we hypothesized that synaptopathy could impair coding of suprathreshold tones to a greater degree because synaptopathic noise exposure affects primarily high-threshold/low-SR ANFs (Furman et al., 2013), which project preferentially to CN SCs (Liberman, 1991; Ryugo, 2008). We therefore plotted the supra-threshold TIN response functions for each neuron, and from these we calculated the mean reduction in spike rate for tones between 80 and 90 dB SPL to designate the supra-threshold impairment of TIN functions (SITIN) (Fig. 3*A*). Mean synapse counts for each animal were calculated across the three cochlear frequencies evaluated (12, 16 and 20 kHz) and used as a single metric for synaptopathy in each animal.
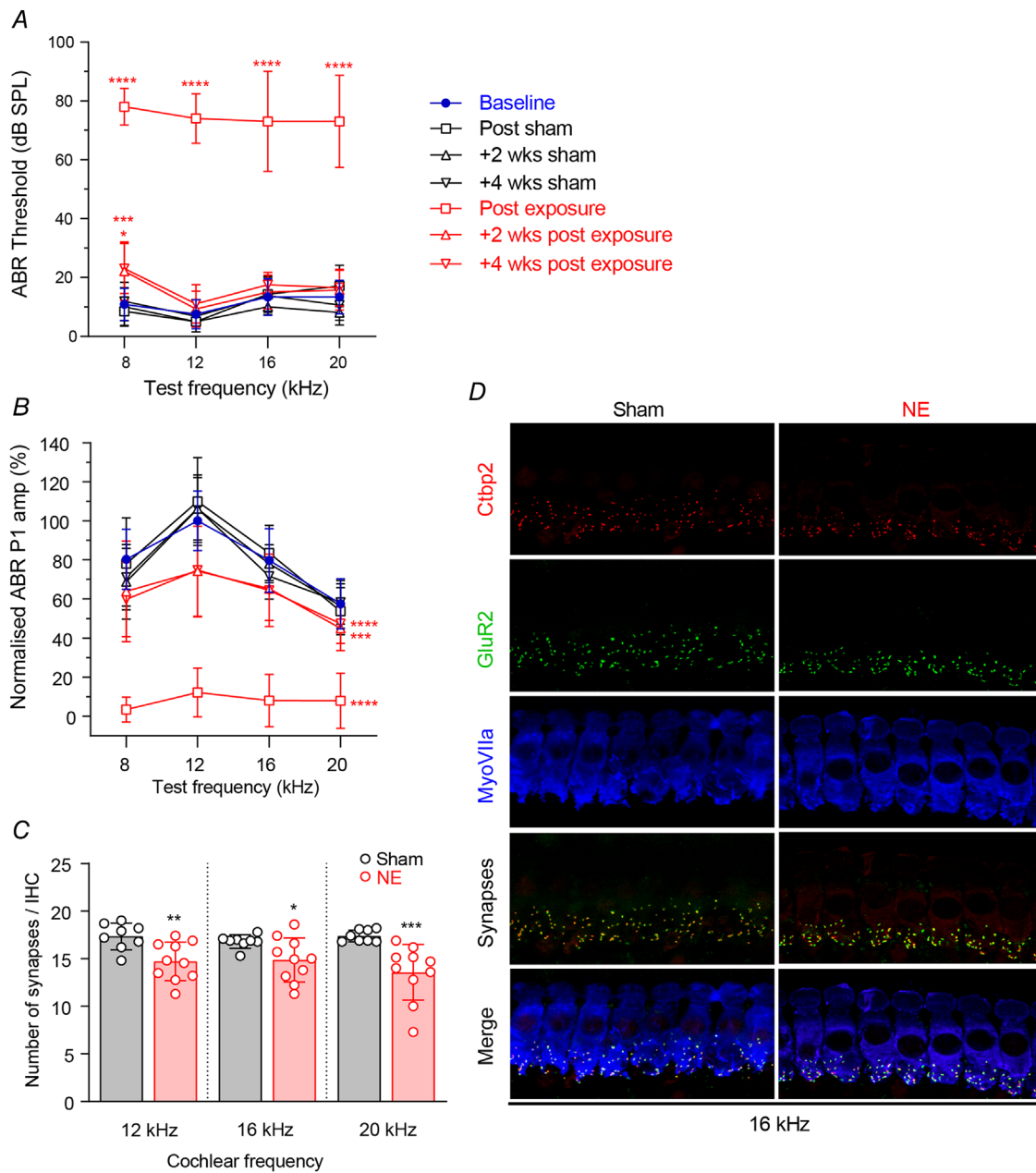
Figure 1. Auditory brainstem response recordings and synapse counts are consistent with inner hair cell synaptopathy

A, noise exposure (NE) produced a temporary threshold shift at mid-to-high frequencies and a mild permanent threshold shift at 8 kHz. *B*, noise exposure resulted in a permanent decrease in mean auditory brainstem response (ABR) wave 1 amplitudes. *C*, acoustic trauma produced a significant decrease in inner hair cell (IHC) synapse density in the noise-exposed animals compared with sham-exposed animals at frequencies above the noise exposure spectrum (17.2% at 12 kHz, 11.3% at 16 kHz and 21.8% at 20 kHz; $P = 0.0092$, $P = 0.0459$ and $P = 0.0003$, respectively). *D*, example synapse immunostaining for a sham- and a noise-exposed animal at the 16 kHz tonotopic cochlea location. For synapse counts, Ctbp2 (ribbon synapses marker, red) and GluR2 (post synaptic marker, green) puncta in each of three adjacent image stacks were captured. Synaptic counts of each *z*-stack were divided by the number of IHCs (visualized by staining with MyoVIIa, blue). Each individual image usually contained 8−10 IHCs. *P < 0.05, **P < 0.01, ***P < 0.001 and ****P < 0.0001. Error bars represent SD. [Colour figure can be viewed at wileyonlinelibrary.com]
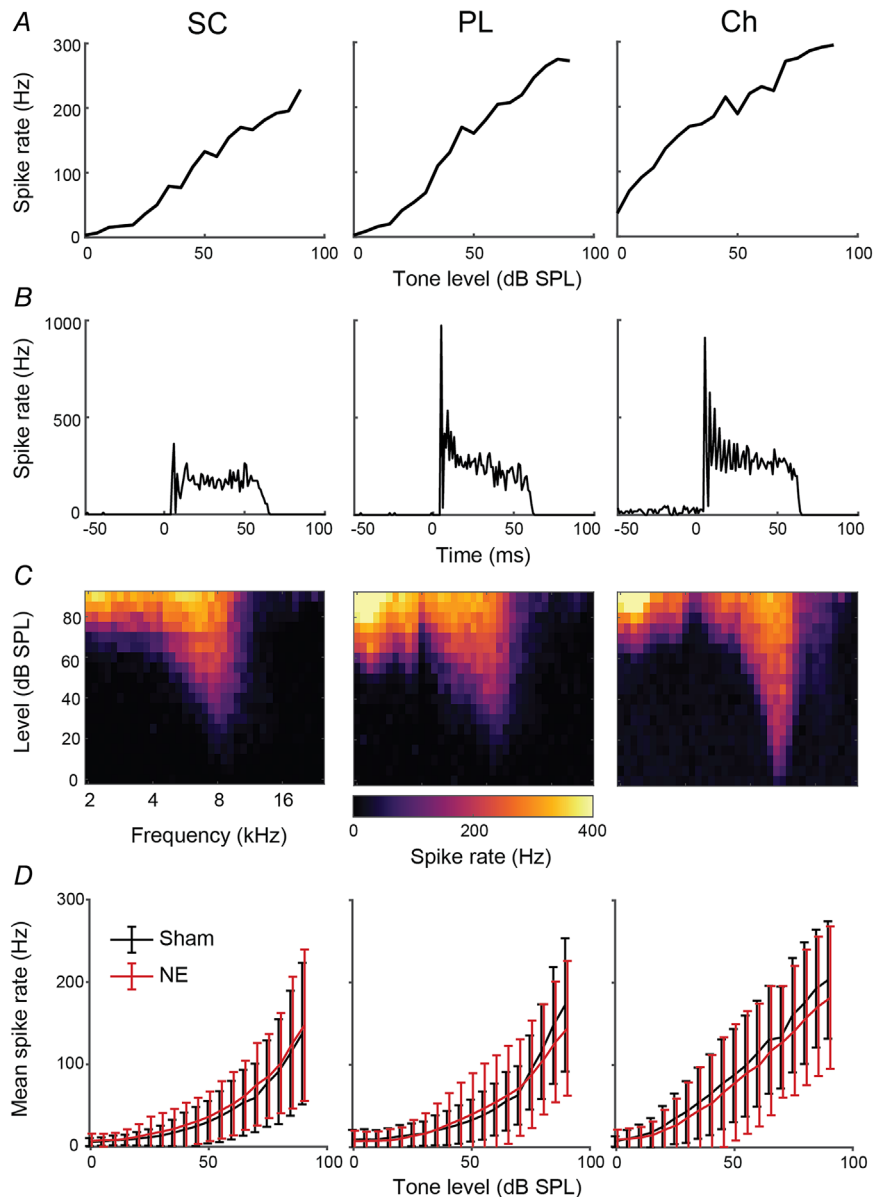
Figure 2. Example cell types of the cochlear nucleus

A–C, for the three major types of cells studied [PL (bushy cell), Ch (T-stellate) and SC (small cell)], we show example rate–level functions (RLFs), peristimulus time histograms (PSTHs) and receptive fields (RFs). *D*, mean (±SD) RLFs for the three cell types in sham- *versus* noise-exposed (NE) animals. [Colour figure can be viewed at wileyonlinelibrary.com]

For SCs, suprathreshold impairment of TIN (SITIN) at 40 (SITIN40) and 60 dB (SITIN60) SPL background sound was significantly correlated with cochlear synapse counts (Fig. 3*B*). The PL neurons showed a significant correlation between SITIN40 and synapse counts, but not SITIN60, whereas Ch cells did not show significant correlations (Fig. 3*C* and *D*).

Cochlear nucleus TIN threshold shifts do not increase after synaptopathy

Tone-in-noise stimuli were presented while recording from CN neurons of sham- and noise-exposed animals to determine the effect of synaptopathy on TIN coding in the CN. The TIN stimuli consisted of the full tone-level range

of RF stimuli presented in the presence of continuous 40 or 60 dB SPL broadband noise (*n* = 397 neurons from four noise-exposed animals and 379 neurons from the four sham-exposed animals). Figure 4*A* shows an example SC RF and the effects of 40 and 60 dB SPL background noise. Here, the background noises produce a 10 or 40 dB threshold shift, respectively (Fig. 4*A*).
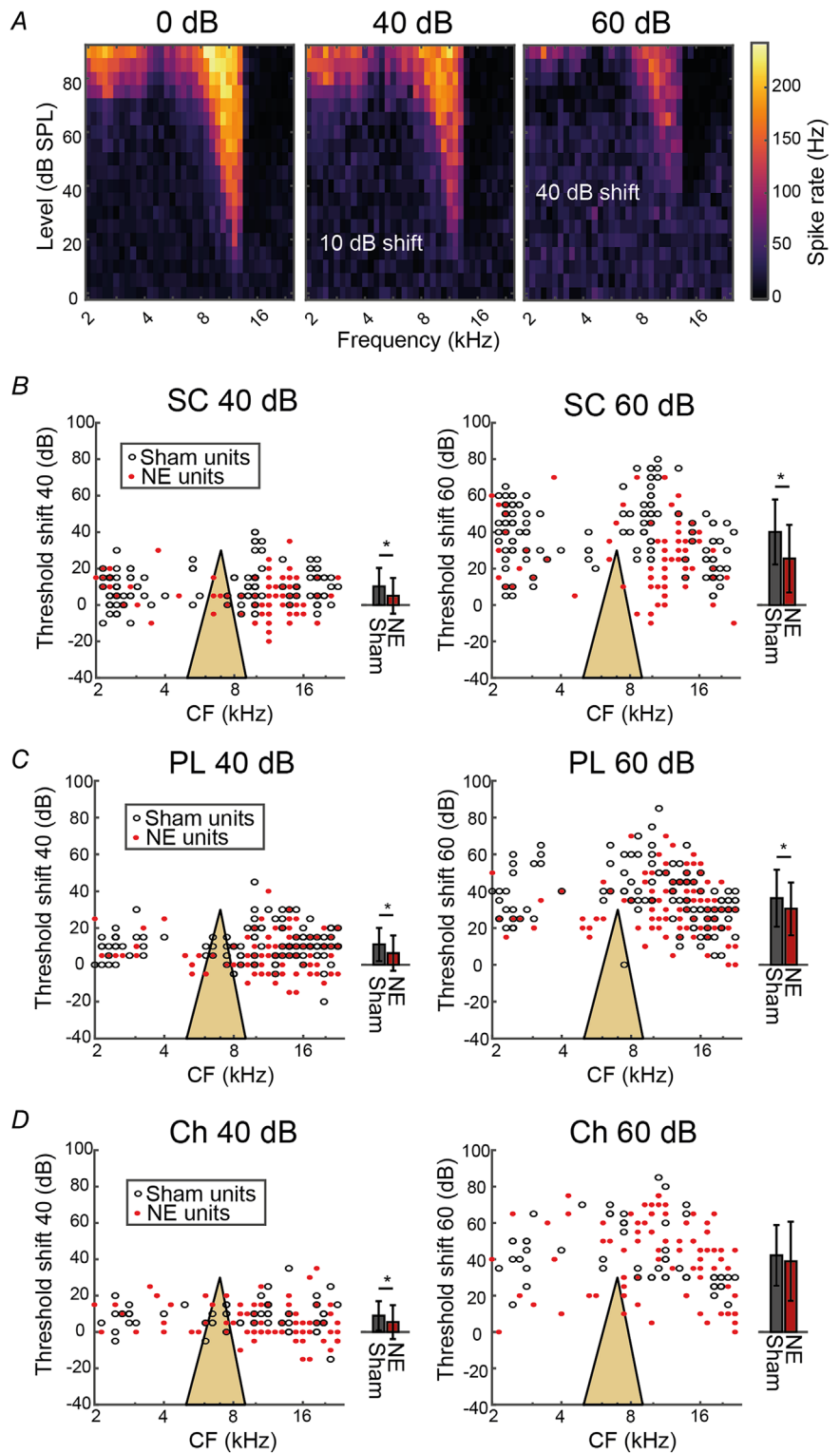
Tone-in-noise threshold shifts for SC, PL and Ch cells are presented in Fig. 4 *B–D*, with a greater TIN threshold shift indicating more impairment of tone perception by the noise. Student's npaired *t* tests revealed that SCs from noise-exposed animals had significantly lower TIN threshold shifts in both background sound levels compared with SCs from sham animals (*n* = 101 NE and 125 sham; *P* < 0.001; Fig. 4*B*). The PL cells from noise-exposed animals also had a significantly lower TIN
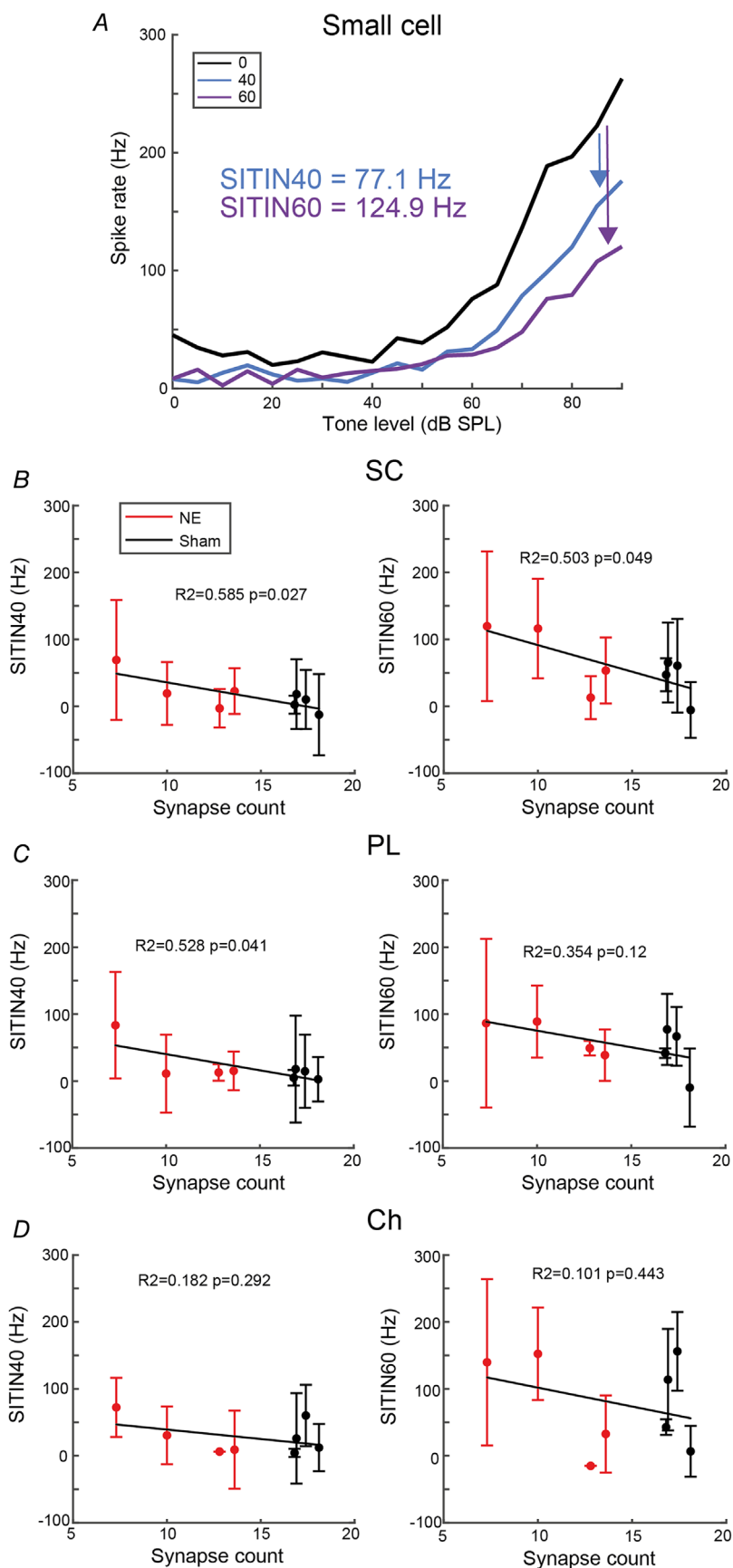
Figure 3. Changes in suprathreshold firing rates in noise are correlated with synaptopathy

A, example singe-neuron suprathreshold impaired tone-in-noise (SITIN) calculation from the rate–level functions of a small cell (SC) from a noise-exposed animal. *B*, SC SITIN is correlated with synaptopathy for 40 and 60 dB background sound levels. *C*, bushy cell (PL) neuron SITIN is correlated with synaptopathy for the lower, but not higher, background sound level. *D*, T-stellate (Ch) neuron SITIN is not correlated with synaptopathy at either background sound level. Error bars indicate SD. [Colour figure can be viewed at wileyonlinelibrary.com]
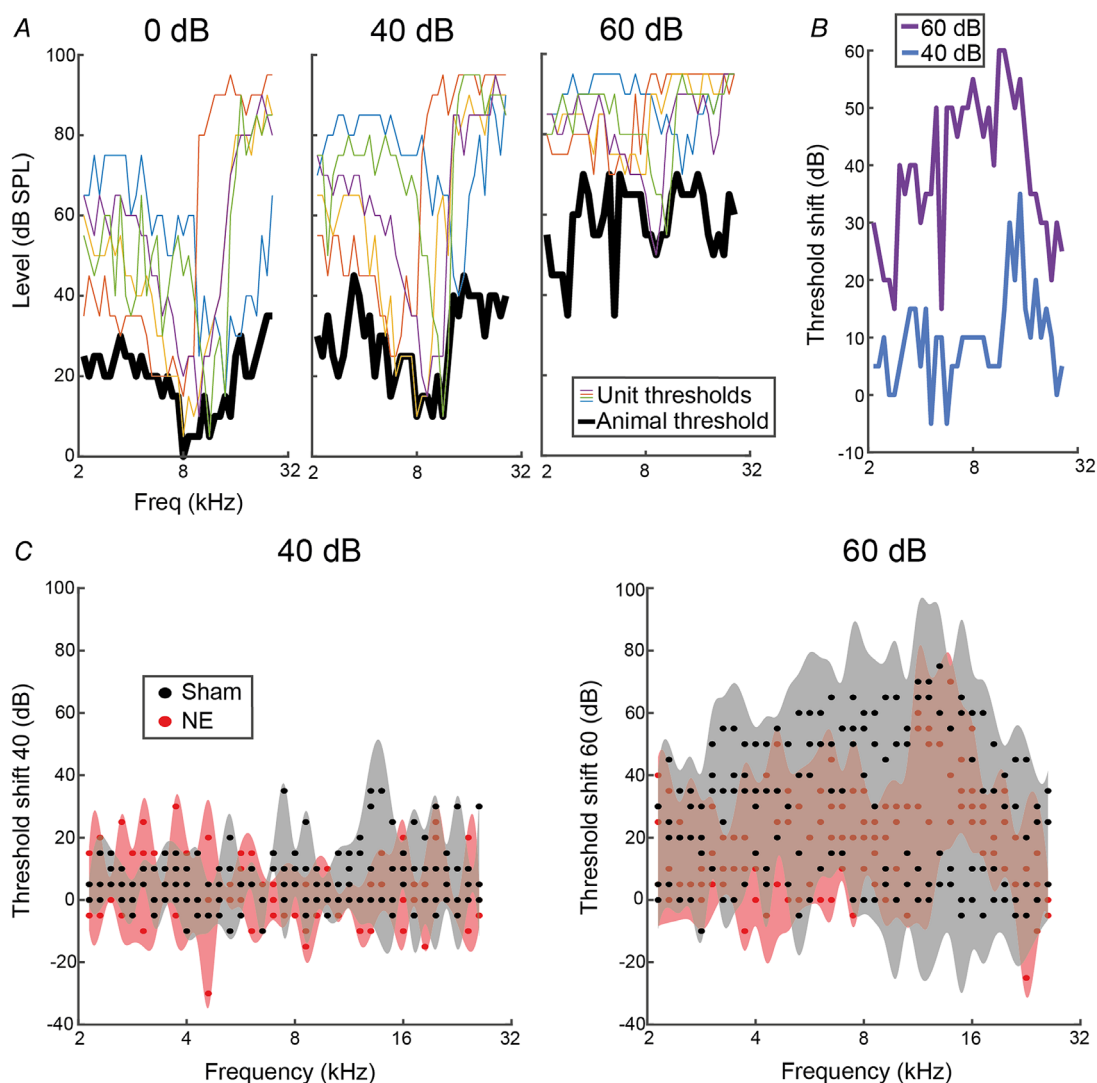
Figure 4. Single-unit tone-in-noise threshold shifts are reduced by cochlear synapopathy

A, example change in receptive field (RF) for a small cell (SC) from a noise-exposed (NE) animal in the presence of 40 and 60 dB SPL background noise. *B*, single-unit tone-in-noise (TIN) threshold shifts for 40 and 60 dB SPL background noise for SCs from sham- and noise-exposed animals. Both individual units (black and red dots) and mean data (±SD, black and red bars) are presented with the same *y*-axis. *C*, single-unit TIN threshold shifts at 40 and 60 dB SPL for bushy cell (PL) neurons from sham- and noise-exposed animals. *D*, single-unit TIN threshold shifts at 40 and 60 dB SPL for T-stellate (Ch) neurons from sham- and noise-exposed animals. Yellow triangles represent the noise exposure spectrum. [Colour figure can be viewed at wileyonlinelibrary.com]

threshold shift than those from sham animals in both 40 and 60 dB SPL background sound levels ($n = 90$ NE and 102 sham; $P = 0.007$ and $P = 0.016$; Fig. 4*C*), but Ch neurons from noise-exposed animals had a significantly lower TIN threshold shift only in 40 dB SPL, but not 60 dB

SPL background sound levels when compared with sham animals ($n = 95$ NE and 58 sham; $P < 0.001$ and $P = 0.525$; Fig. 4*D*). For SCs, this effect was CF specific, with the greatest difference between normal and synaptopathic animals occurring at CFs above the noise exposure

Figure 5. Determining tone-in-noise threshold shifts with estimated audiograms
A, example animal using individual unit thresholds (coloured lines; 5 of 143 units shown for this animal) to estimate the audiometric threshold of animals for tone-in-noise (TIN) stimuli (black). The auditory brainstem response (ABR) thresholds of this animal at 8, 12, 16 and 20 kHz were 10, 5, 15 and 15 dB SPL, respectively. *B*, estimated audiometric threshold shift for this example animal at 40 and 60 dB SPL background noise. *C*, threshold shift of estimated audiometric thresholds in noise for the four sham- and noise-exposed animals. The TIN threshold shifts are equivalent between groups. Shaded area = 95% confidence interval. [Colour figure can be viewed at wileyonlinelibrary.com]

spectrum (Fig. 4*B*), where cochlear synaptopathy is most prevalent (Fig. 1*B* and *C*). In summary, TIN thresholds of single CN neurons are not increased by synaptopathy, signifying no impairment of TIN coding in animals with synaptopathy. Instead, single CN neurons in animals with synaptopathy show reduced TIN threshold shifts.

To confirm the absence of TIN threshold elevations in noise-exposed animals, we used single-unit thresholds to estimate an audiogram for each animal. The outline of the excitatory RF area for every neuron was used to calculate the lowest tone intensity predicted to evoke activity in the CN (Fig. 5*A*). Estimate audiograms are therefore built

using on-CF and off-CF thresholds, allowing assessment of whether off-CF coding might account of the lack of effect observed in the on-CF threshold shift data. We then analysed how the estimated audiometric threshold was shifted in the presence of background noise (Fig. 5*B*). The estimated audiometric TIN threshold shifts reveal limited differences between sham- and noise-exposed animals ($n = 4$ for each group), with a significant difference only at 6.5 kHz for the 40 dB SPL background sound condition, where the shaded 95% confidence interval area does not overlap (Fig. 5*C*). These data are consistent with minimal TIN threshold shifts in the synaptopathy
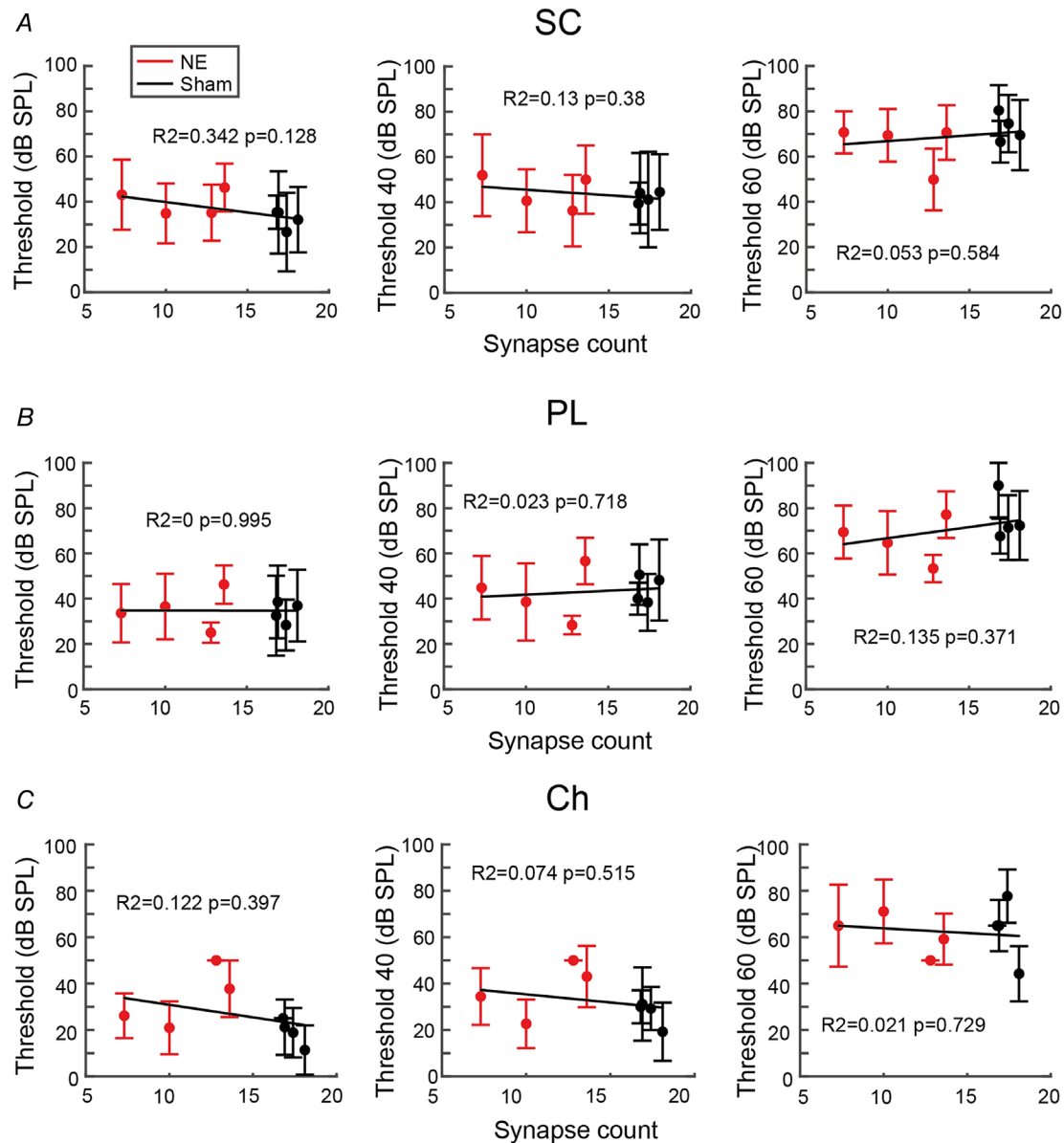
Figure 6. Single-unit thresholds and tone-in-noise thresholds are not correlated with synaptopathy
A, thresholds for small cells (SCs) in the presence of 0, 40 or 60 dB SPL background noise. *B*, thresholds for bushy cell (PL) neurons in the presence of 0, 40 or 60 dB SPL background noise. *C*, thresholds for T-stellate (Ch) neurons in the presence of 0, 40 or 60 dB SPL background noise. Error bars indicate SD. No significant correlations were found between cochlear synaptopathy and any threshold or tone-in-noise threshold. [Colour figure can be viewed at wileyonlinelibrary.com]

animals, by demonstrating that off-CF coding of TIN does not account for the lack of effect observed in Fig. 4.

Synaptopathy induced by noise exposure was not entirely consistent across animals; therefore, although there were no group differences in TIN thresholds between the noise- and sham-exposed groups, we probed the hypothesis that those with more synaptopathy would show impaired TIN thresholds. Figure 6 shows correlations between synapse counts and their mean single-unit TIN thresholds. Synapse counts were calculated as the mean number of synapses per IHC across the three cochlear frequencies evaluated (12, 16 and 20 kHz). No cell type had a significant correlation for any condition, solidifying the conclusion that TIN thresholds are not impaired by cochlear synaptopathy. Figure 7 shows correlations between synapse counts and their mean single-unit TIN threshold shifts. This analysis showed no significant correlations with cochlear synaptopathy.
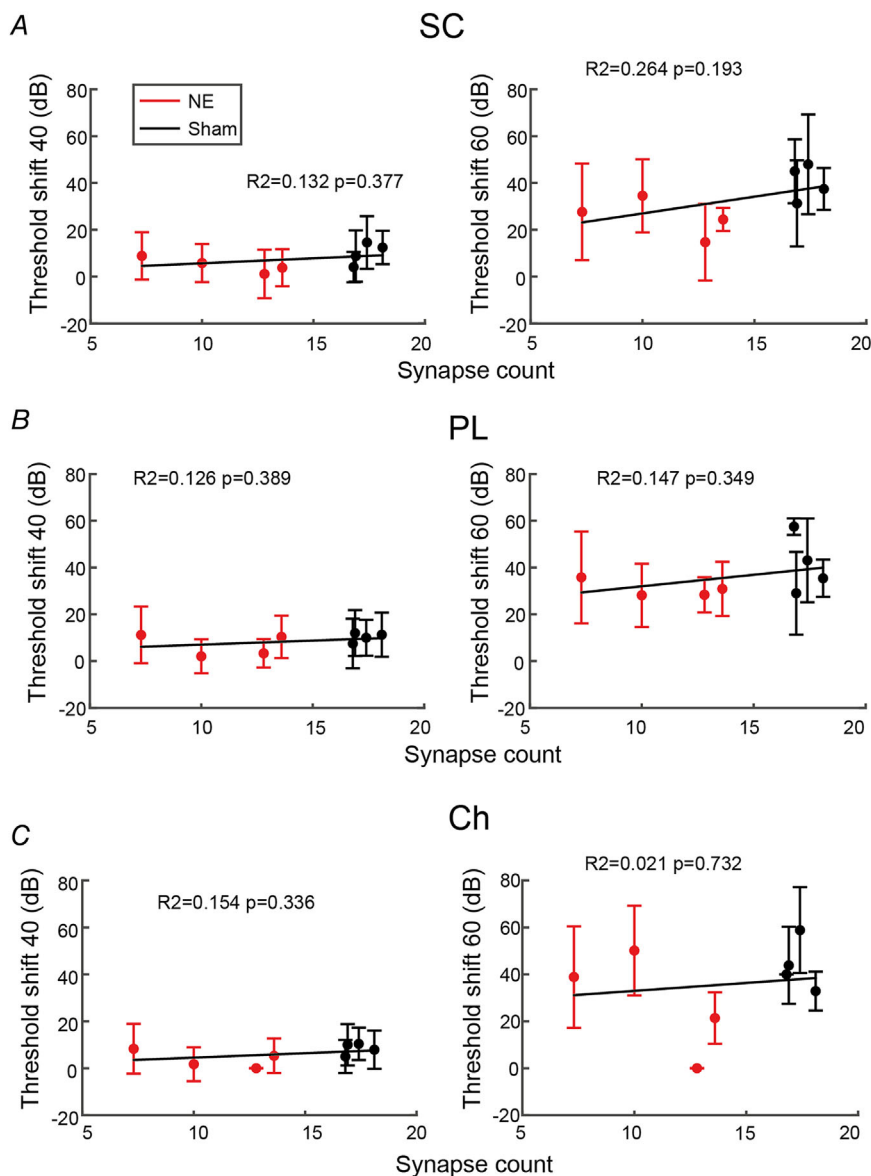
Figure 7. Threshold shifts of cochlear nucleus neurons in the presence of 40 or 60 dB background sound
For small cells (*A*), primary-like neurons (*B*) and chopper neurons (*C*), no significant correlations were found between cochlear synaptopathy and threshold shift in background noise. Error bars indicate SD. [Colour figure can be viewed at wileyonlinelibrary.com]

Cochlear nucleus small cell subtypes

Earlier studies of CN SCs have relied on single-channel recordings, resulting in low numbers of units (Ghoshal & Kim, 1996, 1997). The large number of SCs recorded in the present study with multichannel electrodes gave us the opportunity to test the hypothesis that there might be physiologically heterogeneous groups of SCs (Fig. 8). Rate–level function PCAs were calculated, and k-means clustered using the city block distance metric and repeated for 2–10 clusters. The greatest silhouette score of 0.5161 for two clusters revealed two subtypes of SCs, for which the PC1 metric was binomially distributed, confirming the existence of discrete clusters. Small cell subtype 1 (SC1) was characterized by lower firing rates at high tone intensities and by higher steady-state firing rates compared with onset firing rates. Small cell subtype 2

(SC2) had greater evoked firing rates and unusual onset peaks, with one delayed onset peak at ∼15 ms. Small cell subtype 1 showed a significant correlation between cochlear synapse counts and threshold shifts in 60 dB SPL noise, suggesting that SC1 is responsible for the trend observed in Figs 6 and 7. Neither subtype showed a significant correlation between synapse counts and supra-threshold TIN impairments, suggesting that both cell types contribute to the correlation found in Fig. 3.

Discussion

The data presented here represent the first study on the effects of cochlear synaptopathy on sound coding by cells in the CN. Given that IHC synapse loss cannot currently be quantified in humans, recordings from the guinea pig
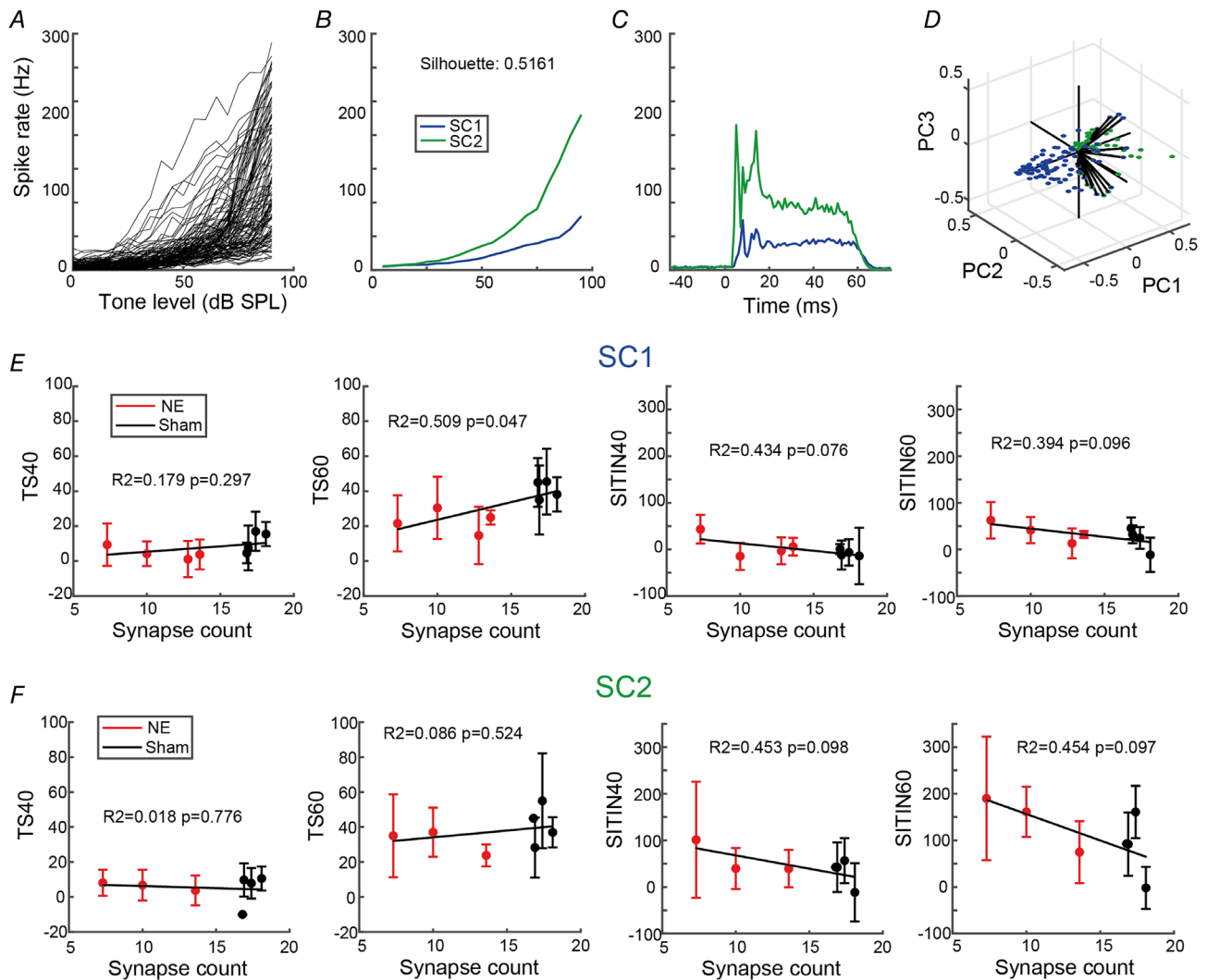
Figure 8. Potential small cell subtypes are both affected by synaptopathy
A–D, based on rate–level function (RLF) shape, small cells (SCs) were categorized into two subtypes (SC1 and SC2) using principal components analysis clustering with different mean RLFs and PSTHs (*B* and *C*). *E* and *F*, subtypes SC1 and SC2, despite their differences in activity patterns, do not show significant correlations between SITIN and synaptopathy. SC1 showed a correlation between synaptopathy and threshold shift, suggesting that SC1s are the drivers of the trend for SCs observed in Fig. 3. Error bars indicate SD. [Colour figure can be viewed at wileyonlinelibrary.com]

CN with induced cochlear synaptopathy were used to determine whether synaptopathy affected sound-evoked thresholds and suprathreshold central responses with and without background noise. We found that TIN detection thresholds were not affected by cochlear synaptopathy. However, suprathreshold TIN coding was impaired in animals with cochlear synaptopathy. The impairments discovered here deepen our understanding of central changes following damage to the auditory periphery and have implications for development of future tests for cochlear synaptopathy in humans.

The noise-exposure model used here produced cochlear synaptopathy with minimal auditory threshold shift at the noise exposure frequency (Fig. 1); however,

whether this would translate to an increased behavioural detection threshold is unknown. Comparisons of ABR thresholds and behavioural detection thresholds have generated variable results, with initial studies showing good correlations between the two measures in noise- and kanamycin-exposed animals (Borg & Engstrom, 1983). However, other studies have shown more variable results, especially for the tone-evoked ABRs as used in this study (Heffner et al., 2008). A more recent study using ouabain-induced cochlear neural degeneration has demonstrated a 30 dB ABR threshold shift with no change to behavioural tone detection thresholds (Resnik & Polley, 2021). Therefore, we do not see the mild permanent threshold shift as a confounding factor in this study,

because behavioural detection thresholds are probably not increased. Cochlear synapse recovery in the guinea pig after synaptopathic noise exposure is well documented (Hickman et al., 2021; Shi et al., 2013; Zhang et al., 2020); therefore, the noise exposure was titrated carefully to ensure that synaptopathy was maintained for ≥4 weeks. The use of anaesthesia during noise exposure affects the damage induced, which might have contributed to the need for a lower exposure level in the present study when compared with other studies of cochlear synaptopathy in guinea pigs (Hickman et al., 2021; Shi et al., 2013; Zhang et al., 2020). These studies have each used different sound levels, frequency spectra and methods for determining hearing thresholds, hence direct comparisons are not straightforward. Initial attempts to titrate our sound exposure level used a lower exposure intensity of 99 dB SPL that resulted in a synapse loss that recovered between 2 and 4 weeks post-exposure, alongside a full recovery of ABR wave 1 amplitudes to baseline levels (data not shown). Increasing the levels enabled us to induce synaptopathy that lasted ≥4 weeks, but we were not able easily to produce a permanent synaptopathy combined with no permanent ABR threshold shift.

Noise exposure produces cochlear synaptopathy that preferentially targets the low-SR/high-threshold ANFs, which is expected to produce difficulty in encoding suprathreshold sounds (Furman et al., 2013). Suprathreshold TIN coding in ANFs occurs to a greater extent in the low-SR fibres owing to flattened RLFs and reduced dynamic ranges in the low-threshold, high-SR fibres (Costalupes et al., 1984; Young & Barta, 1986). The spike-rate code has been shown to be the driving factor for TIN detection in high-frequency ANFs (>2.7 kHz), whereas low-frequency TIN coding uses a temporal code (Huet et al., 2018). For the present study, it is likely that the rate-based intensity code is preserved, because almost all recorded neurons were within the high-frequency region used by a previous study (Huet et al., 2018).

Impairment of suprathreshold sound encoding by cochlear synaptopathy has been assumed to be amplified by central synapse changes following peripheral damage, as has been observed following age-related hearing loss (Wang et al., 2021). However, our data showed no changes to mean RLFs, an unexpected result indicating no impairment of suprathreshold tone coding in the CN. This challenges the hypothesis that reduced input during sound stimulation results in lower spike rates in the VCN. Various homeostatic plasticity mechanisms in the VCN and SCC, including olivocochlear contributions (Hockley et al., 2022), could be responsible maintaining the firing rates observed in the present study (Gröschel et al., 2014; Hockley et al., 2020; Poveda et al., 2020; Vogler et al., 2011). An alternative mechanism is local stress peptide signalling. Pagella et al. (2021) showed that small cells express CRFR2, a urocortin 3 (UCN3) receptor, which

can be produced by bushy and stellate cells. However, the contribution of this peptide on small cell activity or auditory signal processing is currently unknown.

Cochlear nucleus SCs showed the greatest impairment of suprathreshold TIN coding. Small cells receive exclusive input from the low- and medium-SR ANFs, which are preferentially affected by cochlear synaptopathy (Liberman, 1991; Ryugo, 2008). As a result of combined low-SR ANF and olivocochlear collateral inputs, SCs have superior intensity-coding capabilities compared with other CN cell types (Hockley et al., 2022). Therefore, impairment of suprathreshold coding of TIN in SCs might be attributable to changes in low-SR ANF input targeted to SCs or changes to the olivocochlear system following noise exposure.

Small cells project directly to the auditory thalamus, a pathway for short-latency relay of sound intensity information to the auditory cortex, bypassing the inferior colliculus (IC) (Malmierca et al., 2002; Schofield, Mellott et al., 2014; Schofield, Motts et al., 2014). Thus, because the suprathreshold impairments observed here are maximal in SCs they are likely to have a rapid perceptual effect.

Suprathreshold TIN responses are reduced in the CN following synaptopathy. This is counter to results observed in the IC, where increased responses to quiet speech-in-noise are observed (Monaghan et al., 2020). Interestingly, this increased activity occurs only at quiet speech levels, in contrast to the present data, where we see greater reductions to tone-in-noise spike rates at higher tone intensities. Together, these results imply that mechanisms producing increased responses to quiet in noise within the IC occur independently of the effects seen in the VCN and SCC, either in the IC or in other areas that project directly to the IC, such as the DCN. The finding of opposite results in the IC and CN SCs (which bypass the IC) suggests two potential mechanisms for suprathreshold impairment following synaptopathy. Either impairment of SC suprathreshold responses or impairment of central gain mechanisms in the DCN–IC pathway could produce perceptual deficits. It is also possible that the levels used in the present study were not sufficiently high to produce the observed effects in the psychophysical studies.

The data presented here provide clues for identifying cochlear synaptopathy in humans. Although a previous study has shown impaired TIN thresholds in aged humans, the effect was greater at lower background sound intensities (Ralli et al., 2019). We have shown that TIN thresholds in the CN are not altered with synaptopathy, but instead the suprathreshold coding of TIN is affected, suggesting that clinical testing of TIN thresholds is not likely to detect cochlear synaptopathy. Thresholds are instead encoded by the high-SR ANFs, which are not as affected by synaptopathy. Assessing the perceived loudness of suprathreshold TIN stimuli would be more likely to identify synaptopathy in human patients.

References

Borg, E., & Engstrom, B. (1983). Hearing thresholds in the rabbit: A behavioral and electrophysiological study. *Acta Oto-Laryngologica*, **95**(1–4), 19–26.

Costalupes, J. A., Young, E. D., & Gibson, D. J. (1984). Effects of continuous noise backgrounds on rate response of auditory nerve fibers in cat. *Journal of Neurophysiology*, **51**(6), 1326–1344.

Couth, S., Prendergast, G., Guest, H., Munro, K. J., Moore, D. R., Plack, C. J., Ginsborg, J., & Dawes, P. (2020). Investigating the effects of noise exposure on self-report, behavioral and electrophysiological indices of hearing damage in musicians with normal audiometric thresholds. *Hearing Research*, **395**, 108021.

Furman, A. C., Kujawa, S. G., & Liberman, M. C. (2013). Noise-induced cochlear neuropathy is selective for fibers with low spontaneous rates. *Journal of Neurophysiology*, **110**(3), 577–586.

Ghoshal, S., & Kim, D. O. (1996). Marginal shell of the anteroventral cochlear nucleus: intensity coding in single units of the unanesthetized, decerebrate cat. *Neuroscience Letters*, **205**(2), 71–74.

Ghoshal, S., & Kim, D. O. (1997). Marginal shell of the anteroventral cochlear nucleus: Single-unit response properties in the unanesthetized decerebrate cat. *Journal of Neurophysiology*, **77**(4), 2083–2097.

Gröschel, M., Ryll, J., Gotze, R., Ernst, A., & Basta, D. (2014). Acute and long-term effects of noise exposure on the neuronal spontaneous activity in cochlear nucleus and inferior colliculus brain slices. *BioMed Research International*, **2014**, 909260.

Guest, H., Munro, K. J., Prendergast, G., Millman, R. E., & Plack, C. J. (2018). Impaired speech perception in noise with a normal audiogram: No evidence for cochlear synaptopathy and no relation to lifetime noise exposure. *Hearing Research*, **364**, 142–151.

Heffner, H. E., Koay, G., & Heffner, R. S. (2008). Comparison of behavioral and auditory brainstem response measures of threshold shift in rats exposed to loud sound. *The Journal of the Acoustical Society of America*, **124**(2), 1093–1104.

Henry, K. S., & Abrams, K. S. (2021). Normal tone-in-noise sensitivity in trained budgerigars despite substantial auditory-nerve injury: No evidence of hidden hearing loss. *Journal of Neuroscience*, **41**(1), 118–129.

Hickman, T. T., Hashimoto, K., Liberman, L. D., & Liberman, M. C. (2021). cochlear synaptic degeneration and regeneration after noise: Effects of age and neuronal subgroup. *Frontiers in Cellular Neuroscience*, **15**, 684706.

Hockley, A., Berger, J. I., Smith, P. A., Palmer, A. R., & Wallace, M. N. (2020). Nitric oxide regulates the firing rate of neuronal subtypes in the guinea pig ventral cochlear nucleus. *European Journal of Neuroscience*, **51**(4), 963–983.

Hockley, A., Wu, C., & Shore, S. E. (2022). Olivocochlear projections contribute to superior intensity coding in cochlear nucleus small cells. *The Journal of Physiology*, **600**(1), 61–73.

Huet, A., Desmadryl, G., Justal, T., Nouvian, R., Puel, J.-L., & Bourien, J. (2018). The interplay between spike-time and spike-rate modes in the auditory nerve encodes tone-in-noise threshold. *The Journal of Neuroscience*, **38**(25), 5727–5738.

Liberman, M. C. (1991). Central projections of auditory-nerve fibers of differing spontaneous rate. I. Anteroventral cochlear nucleus. *Journal of Comparative Neurology*, **313**(2), 240–258.

Lobarinas, E., Spankovich, C., & Le Prell, C. G. (2017). Evidence of "hidden hearing loss" following noise exposures that produce robust TTS and ABR wave-I amplitude reductions. *Hearing Research*, **349**, 155–163.

Makary, C. A., Shin, J., Kujawa, S. G., Liberman, M. C., & Merchant, S. N. (2011). Age-related primary cochlear neuronal degeneration in human temporal bones. *JARO – Journal of the Association for Research in Otolaryngology*, **12**(6), 711–717.

Malmierca, M. S., Merchán, M. A., Henkel, C. K., & Oliver, D. L. (2002). Direct projections from cochlear nuclear complex to auditory thalamus in the rat. *Journal of Neuroscience*, **22**(24), 10891–10897.

Monaghan, J. J. M., Garcia-Lazaro, J. A., McAlpine, D., & Schaette, R. (2020). Hidden hearing loss impacts the neural representation of speech in background noise. *Current Biology*, **30**(23), 4710–4721.e4.

Pagella, S., Deussing, J. M., & Kopp-Scheinpflug, C. (2021) Expression patterns of the neuropeptide urocortin 3 and its receptor CRFR2 in the mouse central auditory system. *Frontiers in Neural Circuits*, **15**, 747472.

Palmer, A. R. (1987). Physiology of the cochlear nerve and cochlear nucleus. *British Medical Bulletin*, **43**(4), 838–855.

Parthasarathy, A., & Kujawa, S. G. (2018). Neurobiology of disease synaptopathy in the aging cochlea: Characterizing early-neural deficits in auditory temporal envelope processing. *Journal of Neuroscience*, **38**(32), 7108–7119.

Pichora-Fuller, M. K., & Souza, P. E. (2003). Effects of aging on auditory processing of speech. *International Journal of Audiology*, **42**(2), 2S11–6.

Poveda, C., Valero, M., Pernia, M., Alvarado, J., Ryugo, D., Merchan, M., & Juiz, J. (2020). Expression and localization of Kv1.1 and Kv3.1b potassium channels in the cochlear nucleus and inferior colliculus after long-term auditory deafferentation. *Brain Sciences*, **10**(1), 35.

Rajan, R., & Cainer, K. E. (2008). Ageing without hearing loss or cognitive impairment causes a decrease in speech intelligibility only in informational maskers. *Neuroscience*, **154**(2), 784–795.

Ralli, M., Greco, A., De Vincentiis, M., Sheppard, A., Cappelli, G., Neri, I., & Salvi, R. (2019). Tone-in-noise detection deficits in elderly patients with clinically normal hearing. *American Journal of Otolaryngology - Head and Neck Medicine and Surgery*, **40**(1), 1–9.

Resnik, J., & Polley, D. B. (2021). Cochlear neural degeneration disrupts hearing in background noise by increasing auditory cortex internal noise. *Neuron*, **109**(6), 984–996.e4.

Robert Frisina, D., & Frisina, R. D. (1997). Speech recognition in noise and presbycusis: Relations to possible neural mechanisms. *Hearing Research*, **106**(1–2), 95–104.

Ryugo, D. K. (2008). Projections of low spontaneous rate, high threshold auditory nerve fibers to the small cell cap of the cochlear nucleus in cats. *Neuroscience*, **154**(1), 114–126.

Schofield, B. R., Mellott, J. G., & Motts, S. D. (2014). Sub-collicular projections to the auditory thalamus and collateral projections to the inferior colliculus. *Frontiers in Neuroanatomy*, **8**(70), 1–16.

Schofield, B. R., Motts, S. D., Mellott, J. G., & Foster, N. L. (2014). Projections from the dorsal and ventral cochlear nuclei to the medial geniculate body. *Frontiers in Neuro-anatomy*, **8**(10), 1–12.

Sharma, K., Seo, Y. W., & Yi, E. (2018) 'Differential expression of Ca^{2+}-buffering protein calretinin in cochlear afferent fibers: A possible link to vulnerability to traumatic noise', *Experimental Neurobiology*, **27**(5), 397–407.

Shi, L., Liu, L., He, T., Guo, X., Yu, Z., Yin, S., & Wang, J. (2013). Ribbon synapse plasticity in the cochleae of guinea pigs after noise-induced silent damage. *PLoS One*, **8**(12), e81566.

Stabler, S. E., Palmer, A. R., & Winter, I. M. (1996). Temporal and mean rate discharge patterns of single units in the dorsal cochlear nucleus of the anesthetized guinea pig. *Journal of Neurophysiology*, **76**(3), 1667–1688.

Viana, L. M., O'Malley, J. T., Burgess, B. J., Jones, D. D., Oliveira, C. A. C. P., Santos, F., Merchant, S. N., Liberman, L. D., & Liberman, M. C. (2015). Cochlear neuropathy in human presbycusis: confocal analysis of hidden hearing loss in post-mortem tissue HHS Public Access. *Hearing Research*, **327**, 78–88.

Vogler, D. P., Robertson, D., & Mulders, W. H. A. M. (2011). Hyperactivity in the ventral cochlear nucleus after cochlear trauma. *Journal of Neuroscience*, **31**(18), 6639–6645.

Wan, G., Gómez-Casati, M. E., Gigliello, A. R., Liberman, M. C., & Corfas, G. (2014). Neurotrophin-3 regulates ribbon synapse density in the cochlea and induces synapse regeneration after acoustic trauma. *ELife*, **3**, e03564.

Wang, M., Zhang, C., Lin, S., Wang, Y., Seicol, B. J., Ariss, R. W., & Xie, R. (2021). Biased auditory nerve central synaptopathy is associated with age-related hearing loss. *Journal of Physiology*, **599**(6), 1833–1854.

Winter, I. M., & Palmer, A. R. (1995). Level dependence of cochlear nucleus onset unit responses and facilitation by second tones or broadband noise. *Journal of Neuro-physiology*, **73**(1), 141–159.

Wu, P. Z., Liberman, L. D., Bennett, K., de Gruttola, V., O'Malley, J. T., & Liberman, M. C. (2019). Primary neural degeneration in the human cochlea: Evidence for hidden hearing loss in the aging ear. *Neuroscience*, **407**, 8–20.

Young, E. D., Robert, J. M., & Shofner, W. P. (1988). Regularity and latency of units in ventral cochlear nucleus: Implications for unit classification and generation of response properties. *Journal of Neurophysiology*, **60**(1), 1–29.

Young, E. D., & Barta, P. E. (1986). Rate responses of auditory nerve fibers to tones in noise near masked threshold. *Journal of the Acoustical Society of America*, **79**(2), 426–442.

Zhang, Z., Fan, L., Xing, Y., Wang, J., Aiken, S., Chen, Z., & Wang, J. (2020). Temporary versus permanent synaptic loss from repeated noise exposure in guinea pigs and C57 mice. *Neuroscience*, **432**, 94–103.

Additional information

Data availability statement

Data are available as Supporting Information. MATLAB scripts are available from the authors on request.

Competing interests

The authors declare that the research was conducted in the absence of any commercial or financial relationships that could be construed as a potential conflict of interest. G.C. is a scientific founder of Decibel Therapeutics, has equity interest in the company and has received compensation for consulting. The company was not involved in this study. S.E.S. is co-founder and CSO of Auricle Inc., which was not involved in this study.

Author contributions

A.H., G.C. and S.E.S. designed research; A.H., L.R.C. and M.S. performed research; A.H., S.E.S., G.C. and L.R.C. analysed data; A.H., L.R.C. and S.E.S. wrote the paper. All authors have read and approved the final version of the manuscript and agree to be accountable for all aspects of the work in ensuring that questions related to the accuracy or integrity of any part of the work are appropriately investigated and resolved. All persons designated as authors qualify for authorship, and all those who qualify for authorship are listed.

Supporting information

Additional supporting information can be found online in the Supporting Information section at the end of the HTML view of the article. Supporting information files available:

Statistical Summary Document
Peer Review History